Al_2O_3 dielectric layers on H-terminated diamond: Controlling surface conductivity

Yu Yang,[1] Franz A. Koeck,[1] Maitreya Dutta,[2] Xingye Wang,[3] Srabanti Chowdhury,[2] and Robert J. Nemanich[1]
[1]*Department of Physics, Arizona State University, Tempe, Arizona 85287-1504, USA*
[2]*Department of Electrical and Computer Engineering, University of California, Davis, California 95616, USA*
[3]*School for Engineering of Matter, Transport and Energy, Arizona State University, Tempe, Arizona 85287-6106, USA*

(Received 31 May 2017; accepted 1 October 2017; published online 19 October 2017)

This study investigates how the surface conductivity of H-terminated diamond can be preserved and stabilized by using a dielectric layer with an *in situ* post-deposition treatment. Thin layers of Al_2O_3 were grown by plasma enhanced atomic layer deposition (PEALD) on H-terminated undoped diamond (100) surfaces. The changes of the hole accumulation layer were monitored by correlating the binding energy of the diamond C 1s core level with electrical measurements. The initial PEALD of 1 nm Al_2O_3 resulted in an increase of the C 1s core level binding energy consistent with a reduction of the surface hole accumulation and a reduction of the surface conductivity. A hydrogen plasma step restored the C 1s binding energy to the value of the conductive surface, and the resistance of the diamond surface was found to be within the range for surface transfer doping. Further, the PEALD growth did not appear to degrade the surface conductive layer according to the position of the C 1s core level and electrical measurements. This work provides insight into the approaches to establish and control the two-dimensional hole-accumulation layer of the H-terminated diamond and improve the stability and performance of H-terminated diamond electronic devices. *Published by AIP Publishing.* https://doi.org/10.1063/1.4985808

I. INTRODUCTION

Diamond is an ultrawide band gap semiconductor with properties appropriate for high-frequency and high-power electronic devices; its wide band gap (5.47 eV) will sustain a high breakdown field; its high hole-mobility [3800 $cm^2/(V\cdot s)$] results in a low forward resistance; its high saturated drift velocity (1×10^7 cm/s) supports high frequency operation; and its high thermal conductivity [22 W/(cm·K)] enables high power operation.[1] However, due to the large activation energies of dopants, specifically 0.37 eV for p-type doping with boron, the activation fraction of boron in diamond is less than $1/10^4$ at room temperature.[2] A recent research employing dielectric layers on H-terminated diamond has shown breakthroughs in high voltage and high frequency field effect transistor (FET) operation.[3–6] As an alternative doping strategy, studies have employed charge transfer on H-terminated diamond surfaces to form a surface conductive layer with a high density of holes. With air exposure, holes accumulate at the H-terminated diamond surface achieving a hole density of 10^{12}–10^{13} cm^{-2} and hole mobility of 50–150 $cm^2/(V\cdot s)$.[7]

Several mechanisms have been proposed to explain how H-termination enables the surface hole accumulation layer that leads to the surface conductivity. The electrochemical surface transfer doping model is now well accepted over other competing models. In this model, after charge transfer, the Fermi level of the adsorbate layer and the diamond are aligned, resulting in a layer of accumulated holes at the diamond surface and an equal density of compensating negative charges in the adsorbates.[8] However, there is still disagreement on the specific molecules that are most effective in forming the air-induced surface conductivity. There is upward band bending in the diamond, and the Fermi level is near the valence band maximum (VBM) at the surface. The changes in band bending correspond to the changes in the surface transfer doping. Furthermore, the surface hole density will be reflected in the relative position of the C 1s core level binding energy determined by X-ray photoemission spectroscopy (XPS).[9]

Although surface transfer doping can enable high performance diamond FET operation, the surface conductivity of the air-exposed H-terminated diamond surface is not thermally stable above ~190 °C in vacuum.[10] The atmospheric adsorbates desorb from the surface during heating above room temperature, resulting in a drop of the hole concentration.[11] For electronic device applications, the stability of H-terminated diamond FETs needs to be improved.

Kawarada *et al.* have reported the formation of a surface hole accumulation layer after Al_2O_3 atomic layer deposition (ALD) on diamond surfaces preheated to 450 °C. They suggest that the ambient adsorbates are removed[12] and that the air exposure process is apparently not necessary to obtain surface conductivity in the H-terminated diamond/Al_2O_3 structure. Apparently, dielectric layers, like Al_2O_3, can enable surface conductivity on H-terminated diamond without molecular adsorbates. An indication that this process differs from the air-exposed, H-terminated surface is that the surface conductivity of the dielectric/diamond interface is retained at high temperature (>400 °C).

Various dielectric layers, including SiO_2,[13] Al_2O_3,[14] AlN,[15] HfO_2,[16] $LaAlO_3$,[17] MoO_3,[18] and V_2O_5,[19] which have been used as insulators on the H-terminated diamond

surface, have been deposited by thermal evaporation, thermal atomic layer deposition (ALD), or metal organic chemical vapor deposition (MOCVD).

Plasma enhanced ALD (PEALD) is an energy-enhanced ALD method that has been used to form high quality dielectric layers for semiconductor devices. By using activated oxygen species (e.g., O_2*, O*, and O) generated by a plasma, PEALD enables conformal and uniform amorphous Al_2O_3 film growth with an atomic scale thickness control, a decreased deposition temperature and impurity density, and also an increase of the growth rate and film density compared with chemical vapor deposition (CVD) or thermal ALD.[20,21] However, there have been few results on H-terminated diamond because the oxygen plasma step is thought to degrade the 2D hole accumulation layer in H-terminated diamond.[22] Consequently, we are motivated to investigate how the surface conductivity of H-terminated diamond can be preserved and stabilized by using a dielectric passivation layer with an *in situ* post-deposition treatment.

II. EXPERIMENTAL

Thin layers of Al_2O_3 were deposited on commercially obtained optical grade $4 \times 4\,mm^2$ type IIa CVD single crystalline undoped diamond (100) substrates and $3 \times 3\,mm^2$ type IIa CVD single crystalline diamond (100) substrates with lightly boron doped epitaxial layers. The boron doped layer prepared by Fraunhofer USA was used to mitigate the charging shifts during X-ray photoemission spectroscopy (XPS). The boron concentration was estimated using Fourier transform infrared spectroscopy (FTIR) to be around $5–10 \times 10^{17}\,cm^{-3}$. The thickness of the epitaxial layer was ~6–10 μm.

H-terminated diamond surfaces were achieved in a hydrogen plasma excited with 1000 W microwave input for 15 min at ~800 °C (measured with an optical pyrometer). The chamber pressure was maintained at ~50 Torr with a H_2 flow rate of 400 standard cubic centimeters per minute (sccm). After cooldown, the H-terminated diamond surface was exposed to air for ~12 h to obtain the atmospheric adsorbates responsible for surface conductivity.

Al_2O_3 films were deposited by remote PEALD. The precursor was dimethylaluminum isopropoxide (DMAI, $[(CH_3)_2AlOCH(CH_3)_2]_2$), and oxygen plasma was the oxidizer. The PEALD growth rate was ~1.5 Å/cycle at a substrate temperature of 100 °C. Similarly prepared Al_2O_3 films were shown to be amorphous.[21]

After Al_2O_3 deposition, the surface was processed with a hydrogen plasma post-deposition treatment for 30 min at ~500 °C. The post-deposition hydrogen plasma was excited by a radio frequency (rf) source (100 W, 13.56 MHz) applied to a helical copper coil wrapped around a ~32 mm diameter quartz tube located ~25 cm above the sample. The chamber pressure was maintained at 100 mTorr with a constant gas flow of 20 sccm controlled by a throttle valve in front of the turbo pump.

The hole accumulation layer and the band bending of the diamond surface region was further corroborated using the binding energy of the C 1s core-level. The *in situ* XPS measurements were performed after each process step using a monochromated Al K_α X-ray source ($h\nu = 1486.6$ eV) with a bandwidth of 0.2 eV and a R3000 Scienta analyzer with a resolution of 0.1 eV. All core level spectra were recorded with a 0.05 eV step, and the peak positions can be resolved to $\sim \pm 0.05$ eV by curve fitting.

The method proposed by Waldrop and Grant[23] and Kraut *et al.* was used[24] for determining the valence band offset (VBO). The method is represented in the following equation:

$$\Delta E_V = (E_{CL} - E_V)_{Diamond} - (E_{CL} - E_V)_{Al_2O_3} - \Delta E_{CL}, \quad (1)$$

where ΔE_V represents the VBO; E_{CL} is the binding energy of the XPS core level; E_V is the valence band maximum (VBM); $(E_{CL}\text{-}E_V)_{Diamond}$ or $(E_{CL} - E_V)_{Al_2O_3}$ are the binding energy difference from the VBM to the respective core level; and ΔE_{CL} is the binding energy difference between the diamond and Al_2O_3 core levels measured at the interface $(E_{CL}^{C\,1s}\text{-}E_{CL}^{Al\,2p})$.

The surface conductivity was characterized on $4 \times 4\,mm^2$ type IIa undoped single crystalline diamond (100) substrates by measuring the diagonal resistance and the position of the corresponding C 1s core level. The distance between the two probes was ~5.5 mm. A small piece of gold foil was used under each probe tip to increase the contact area.

III. RESULTS

A. PEALD Al_2O_3 deposition and hydrogen plasma treatment

For the H-terminated diamond surface after air exposure, the C 1s core level binding energy was measured at 284.1 eV. The O 1s core level showed features at 530.4 eV and 532.1 eV, which may originate from C-O bonds and adsorbates, respectively. After deposition of ~1 nm Al_2O_3 on boron doped diamond, the Al 2p core level was clearly observed at 73.7 eV, indicating that a thin Al_2O_3 layer was successfully formed on the diamond. However, the C 1s peak shifted to a higher binding energy of 285.1 eV, indicating a transition from upward band bending to downward band bending and a reduction of the surface hole accumulation density. After hydrogen plasma, the C 1s binding energy was restored to the same level as the conductive diamond surface, while the Al 2p and O 1s core levels shifted to lower binding energy by 1.7 eV and 1.5 eV, respectively. We note that while H-diffusion may occur through the thin film and weak points, the XPS results indicate that the surface is uniformly affected. With the deposition of an additional ~2 nm Al_2O_3, the C 1s remained at 284.1 eV, which is characteristic of the surface conductive state. The C 1s peak was not affected by further Al_2O_3 deposition.

With the application of a hydrogen plasma to the 20 nm Al_2O_3 layer, the Al 2p peak was fit with two peaks at 73.8 eV and 75.1 eV. The double peak was ascribed to Al_2O_3 layers at different depths. The result indicates that the hydrogen plasma treatment affected the surface of the Al_2O_3 layer. Evidently, at different depths, the Al_2O_3 layers had different levels of included charge. Figure 1 shows the C 1s, Al 2p and O1s core levels of the (100) B-doped diamond surface

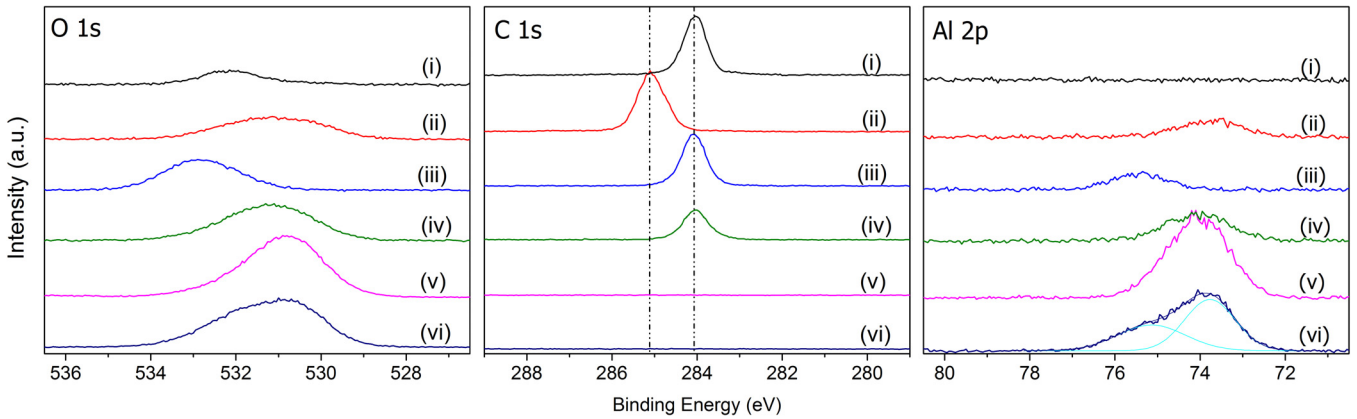

FIG. 1. The respective XPS scans of the O 1s, C 1s, and Al 2p core levels of (i) H-terminated diamond surface with air exposure, (ii) after 1 nm Al_2O_3 deposition, (iii) 500 °C H-plasma treatment, (iv) after 2 nm Al_2O_3 deposition, (v) after 20 nm Al_2O_3 deposition, and (vi) 500 °C H-plasma treatment. (For different elements, the intensity scales are adjusted for better visibility.).

after each process. The XPS core level binding energies are summarized in Table I.

A control experiment was carried out to establish the necessity of the ambient exposure before dielectric layer deposition. A hydrogen plasma process at 500 °C was applied to hydrogenated undoped diamond to remove air-induced adsorbates without destroying the H-termination. After the *in situ* 500 °C, hydrogen plasma process, the C 1s core level shifted from 284.0 eV to 284.2 eV, indicating a change in the band bending, which is presumed to correspond to the removal of air-induced surface conductivity. After 2 nm Al_2O_3 deposition, the C 1s shifted to 285.0 eV. A hydrogen plasma post-deposition process was able to restore the C 1s core level to 284.0 eV. This indicates that air induced adsorbates are not necessary to achieve the surface conductivity of the H-terminated diamond/Al_2O_3 structure.

B. Correlation of binding energy and surface resistance

Figure 2 shows the C 1s core level binding energy and the surface resistance of the $4 \times 4\,mm^2$ undoped diamond after each process. Initially, the H-terminated diamond surface after the air exposure showed a surface resistance of ~30 kΩ, which is consistent with the formation of a surface conductive layer.[25] The corresponding C 1s core level was measured at 284.1 eV. We have observed a small variation of ±0.1 eV in the C 1s core level binding energy of the H-terminated diamond surface with air-induced adsorbates. This variation may relate to the bulk Fermi level of the different diamond substrates. After the first PEALD Al_2O_3 deposition, which employed an oxygen plasma, the surface resistance increased to ~3 MΩ, and the C 1s core level shifted to a higher binding energy of 286.3 eV, indicating the removal of the upward band bending and the surface hole accumulation layer. With hydrogen plasma treatment, the C 1s core level was restored to 284.1 eV, and the diagonal surface resistance decreased to ~20 kΩ. The hydrogen plasma process was able to restore the upward band bending that was apparently removed during the oxygen plasma process. With further PEALD Al_2O_3 deposition, the C 1s core level was not affected, and the surface conductivity was not obviously degraded.

TABLE I. XPS of C 1s, Al 2p, and O 1s core levels results for boron-doped diamond. All values are in units of eV and have an uncertainty of ±0.1 eV.

Process	C 1s	O 1s	Al 2p
H-plasma and air exposure	284.1	530.6 and 532.1	…
1 nm Al_2O_3 deposition	285.1	531.1	73.7
H-plasma	284.1	532.6	75.4
2 nm Al_2O_3 deposition	284.0	521.2	74.1
20 nm Al_2O_3 deposition	…	530.6 and 531.4	74.1
H-plasma	…	530.4 and 531.5	73.8 and 75.1

C. Plasma effects

The oxygen coverage was estimated from the XPS spectra shown in Fig. 3, using the following equation:[26]

$$\Theta_O = \frac{I_O}{S_O} \Big/ \frac{I_C}{S_C} \times \sum_{n=0}^{\infty} \exp\left[\frac{-n \times d_{Diamond}}{\lambda_{Diamond} \times \cos(\varphi)}\right], \quad (2)$$

where Θ_O, the coverage in monolayers (ML), is the number of absorbed O atoms per unit area (atoms/cm^2) divided by the number of surface C atoms per unit area (atoms/cm^2). I_O and I_C are the integrated intensities of the O 1s and C 1s peaks from Fig. 3. S_O and S_C are the atomic sensitivity factors for the O 1s and C 1s photoelectrons; $d_{Diamond}$ is the spacing between two (100) planes, which is 3.57 Å. $\lambda_{Diamond} \approx 18.9$ Å is the inelastic mean free path of C 1s electrons with kinetic energies of ~1200 eV;[27] φ is the angle between the normal direction and the XPS energy analyzer, which is 0° for this setup.

To determine the effects related to oxygen or hydrogen plasma, the processes were successively applied to an H-terminated undoped diamond surface. The oxygen plasma used the chamber for PEALD Al_2O_3 deposition. The oxygen coverage increased from 0.15 ML for an atmosphere exposed H-terminated diamond surface to 0.55 ML after oxygen plasma. The C 1s core level shifted from 283.9 eV for the atmosphere exposed H-terminated surface to 284.3 eV, and the diagonal resistance increased to >1 MΩ. The surface conductivity was apparently destroyed by the oxygen plasma

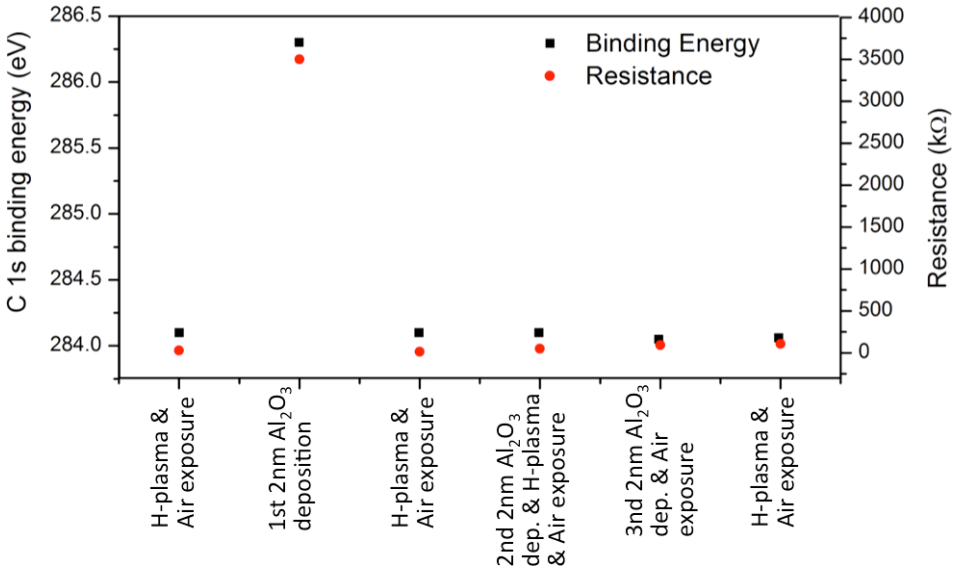

FIG. 2. The C 1s binding energy and resistance of the diamond surface for the different process steps.

process as reported previously.[22] A 500 °C hydrogen plasma treatment identical to that used in the post-deposition treatment was then applied to the air-exposed oxidized surface. A fraction of the oxygen was removed, and the oxygen coverage decreased to ~0.25 ML. The surface conductivity was restored as indicated by the C 1s core level which shifted to 284.0 eV and the diagonal resistance which was reduced to 31.7 kΩ, a value within the range for surface conductive diamond. The hydrogen plasma process was able to remove a fraction of the oxygen atoms at the diamond surface and restore the surface conductivity.

D. Oxide charge state

This section addresses the band shifts that occur in the oxide after various processing steps. The presumption is that charge in the oxide is changed due to diffusion of atoms or molecules into/out of the dielectric layer or due to changing the charge state of diffused species or defects.

For an H-terminated diamond surface with a thin (~2 nm) layer of Al_2O_3 and 500 °C hydrogen plasma treatment, further PEALD Al_2O_3 deposition did not change the C 1s core level. However, with annealing at 500 °C, the Al 2p and O 1s core levels shifted 0.6 eV together to higher binding energy, indicating a downward band shifting of the oxide layer. This result suggests the charge induced by the oxygen plasma could be removed by annealing to 500 °C. With a further 500 °C hydrogen plasma process, the Al 2p and O 1s core levels shifted another 0.6 eV towards higher binding energy further increasing the downward band shifting. The results of the Al 2p, C 1s and O 1s core levels are shown in Fig. 4. The oxygen plasma and hydrogen plasma processes have apparently induced opposite charge into the oxide layer, which resulted in different band shifting.

We now consider the effect of a 500 °C H-plasma process followed by a 500 °C anneal. A diamond surface with an 8 nm Al_2O_3 layer was processed with a 500 °C H-plasma. The C 1s, O 1s, and Al 2p core levels are shown in Fig. 5. After the 30 min 500 °C anneal process, the C 1s was maintained at ~283.9 eV indicating surface conductivity. The O 1s and Al 2p core levels were not affected by the anneal indicating that charges in the oxide layer induced by hydrogen plasma were not affected by the anneal process. The anneal results established that the hydrogen plasma processed interface was apparently thermally stable at 500 °C. This is a notable difference from an air exposed, H-terminated diamond surface.

IV. DISCUSSION

A. Interface model

An interface layer is used to explain the effects of the first and second PEALD Al_2O_3 deposition on the diamond surface

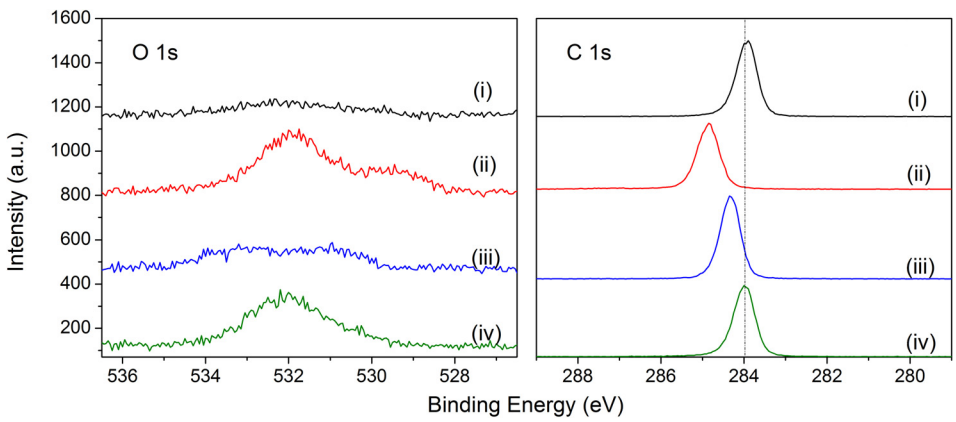

FIG. 3. XPS scans for O 1s and C 1s core levels of (i) H-terminated diamond surface with air exposure, (ii) after oxygen plasma treatment, (iii) after hydrogen plasma treatment, and (iv) air exposure. (For different elements, the intensity scales are adjusted for better visibility.).

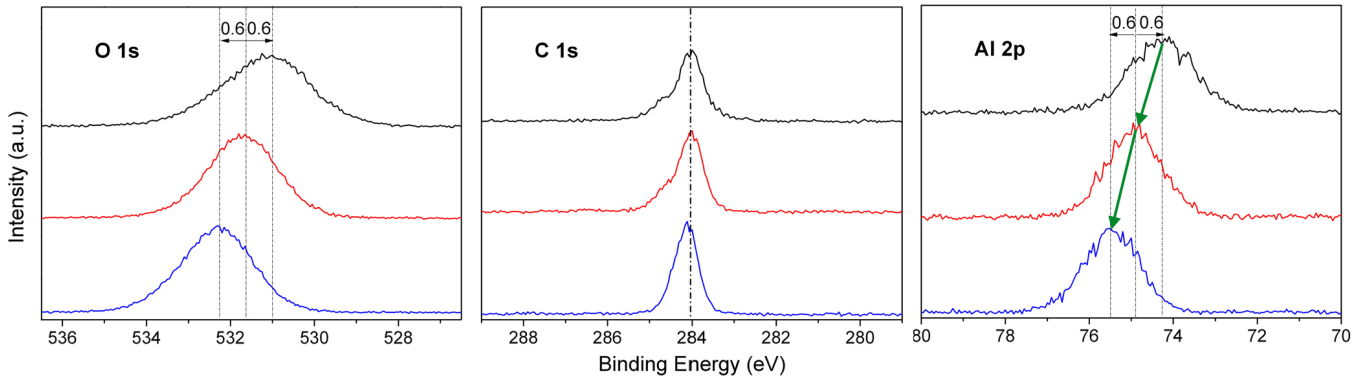

FIG. 4. XPS scans of a diamond surface with a 2 nm layer of Al_2O_3 and hydrogen plasma treatment, showing the O1s, C 1s, and Al 2p core levels after (i) an additional 2 nm PEALD Al_2O_3 deposition [this surface is essentially the same as scan (iv) in Fig. 1], (ii) 500 °C vacuum anneal, and (iii) 500 °C hydrogen plasma process. (For different elements, the intensity scales are adjusted for better visibility.).

conductivity, and post-deposition hydrogen plasma treatment. The effect of the initial H-termination and air exposure was apparently removed by the oxygen plasma during the PEALD process. With post-deposition hydrogen plasma treatment, the surface conductivity is restored. Presumably, hydrogen atoms can diffuse and incorporate into the diamond/Al_2O_3 interface to modify the interface, such that electron transfer is promoted from the diamond valence band into the interface layers. Within this model, the interface layer is charged, as indicated by the large shifts of the C 1s and Al 2p core levels. During the following PEALD process, the interface layer is apparently protected by the initial dielectric layers, and the charge transfer layers are not destroyed by the oxygen plasma during further PEALD cycles.

The air exposure process is apparently not necessary to obtain surface conductivity in the H-terminated diamond/Al_2O_3 structure, as indicated by the results in Sec. IV A. This is consistent with the results of Kawarada *et al*. that showed surface hole accumulation after Al_2O_3 ALD on a diamond surface preheated to 450 °C. In the post-deposition hydrogen plasma treatment, the hydrogen atoms may form interface bonding similar to that of ALD Al_2O_3 on diamond where H_2O is used as oxidant.

B. Band alignment schematics

For application as an FET, it is necessary to obtain interface carrier confinement properties, which are determined by the band offsets. According to Fig. 4, oxygen plasma induced charge resulted in a 0.6 eV shift of the Al 2p core level towards lower binding energy. The VBO between as-grown Al_2O_3 and diamond was determined to be 2.7 eV by using Eq. (1) and taking account of the plasma effects (i.e., 0.6 eV shift observed after thermal annealing). The value of $(E_{CL}\text{-}E_V)_{Al2O3}$ was 70.6 ± 0.1 eV (Ref. 21) and $(E_{CL}\text{-}E_V)_{Diamond}$ was 284.1 ± 0.1 eV. The diamond value was based on the assumption that the VBM is at the Fermi level for the surface conductive state. This band offset value is consistent with other reported results.[28] The band gaps of Al_2O_3 and diamond (5.47 eV) are necessary to calculate the conduction band offset (CBO). A previous study from our group reported the band gap of PEALD Al_2O_3 as 6.7 ± 0.1 eV,[21] which was determined from the energy loss spectrum associated with the XPS O 1s core level. Using 6.7 eV as the band gap of the Al_2O_3 films, the Al_2O_3 conduction-band minimum (CBM) is calculated to be 1.5 eV below the diamond CBM. The deduced band alignment diagram of Al_2O_3 on the diamond is shown in Fig. 6(ii). The diagram shows that Al_2O_3 is able to confine holes but fails to confine electrons for the surface conductive diamond.

Considering a charged interface layer and accounting for the effects of hydrogen and oxygen plasma, the band diagram and the charge transfer for each process step are summarized in Fig. 6. In Fig. 6(i), for air-exposed, H-terminated diamond, electrons transfer from the valence band into the

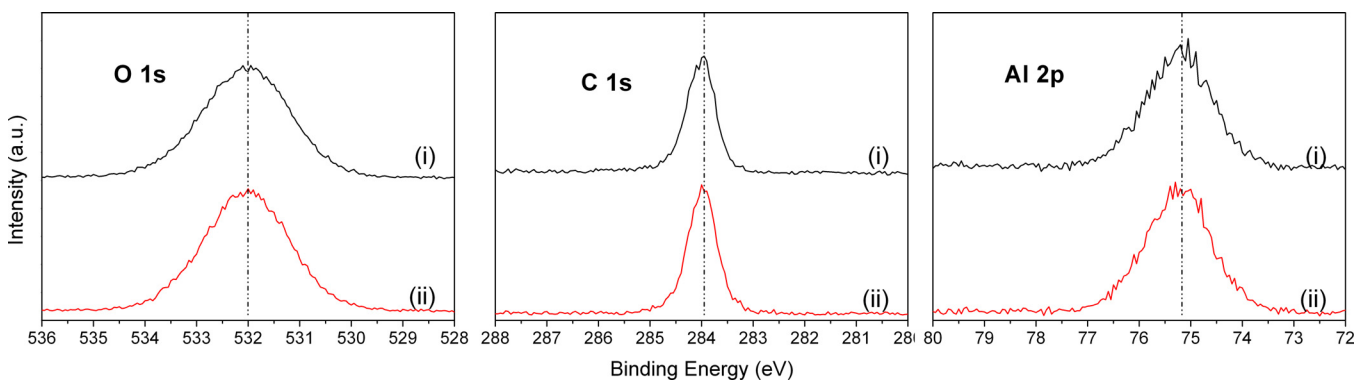

FIG. 5. XPS scans of a diamond surface with a thin layer of Al_2O_3 ~8 nm and hydrogen plasma treatment, showing the O1s, C 1s, and Al 2p core levels (i) before and (ii) after thermal anneal at 500 °C. (For different elements, the intensity scales are adjusted for better visibility.).

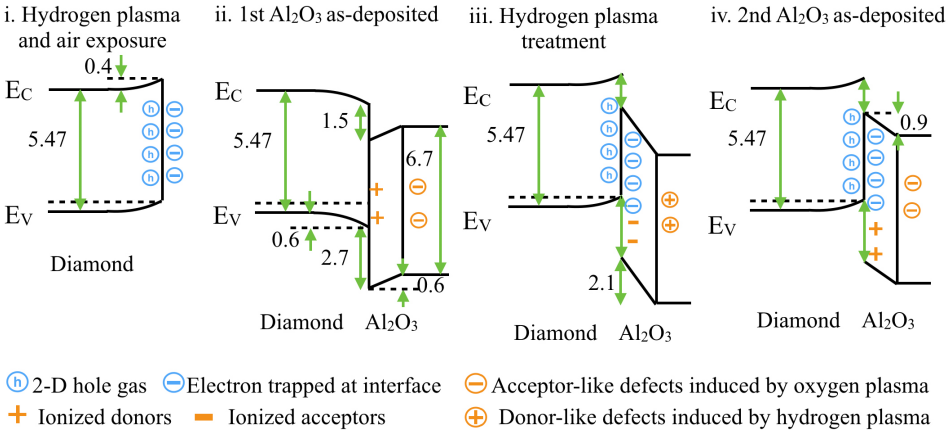

FIG. 6. Interface band diagrams of Al_2O_3 on diamond showing band bending and possible charged states distributions after each process: (i) hydrogen terminated diamond with air exposure, (ii) 1st PEALD Al_2O_3 deposition ~1 nm, (iii) hydrogen plasma treatment at 500 °C, and (iv) 2nd PEALD Al_2O_3 deposition ~2 nm. The charges in the schematic diagram indicate their spatial position, not their energy relative to the band gap.

adsorbate layer, leaving an equal density of holes in the diamond valence band.

After a thin PEALD Al_2O_3 layer, the diamond upward band bending and the hole accumulation was reduced, resulting in the loss of surface conductivity, as shown in Fig. 6(ii). Furthermore, during PEALD, the oxygen plasma process introduces a concentration of defects or interstitial oxygen atoms, which act as electron traps or acceptors in the oxide layer.[21,29] These defects are compensated by ionized impurities or defects in the interface layer. This charge/dipole layer leads to an upward band shift across the interface layer, as shown in Fig. 5(ii). An anneal to 500 °C reduces the upward band shift, which may be due to diffusion and desorption of excess oxygen.

The charge distribution after the post deposition 500 °C hydrogen plasma treatment is shown in Fig. 6(iii). The hydrogen plasma process modifies the interface layer and restores the surface hole accumulation. The electron transfer from the diamond into the interface layer results in a negatively charged interface layer. The holes and electrons at the interface result in upward band bending of the diamond valence band. Moreover, a large downward shift of the oxide core levels is observed. A 500 °C anneal does not reduce this downward band shift. Evidently, the hydrogen plasma process affects the oxide layer oppositely compared to an oxygen plasma. A possible explanation is that the hydrogen plasma introduces donor-like defects into the oxide near the interface layer. These defects contribute negative charge into the interface layer, and the positively charged donor states contribute to a dipole layer that accounts for the shift of the Al_2O_3 bands. It is notable that this configuration is stable during a 500 °C anneal indicating that the diamond/Al_2O_3 interface is more thermally stable compared to the charges trapped in air-induced adsorbates on diamond.

After additional PEALD Al_2O_3, the donor-like defects induced by the hydrogen plasma are removed and replaced with acceptor-like defects. Also, the negative charges that compensate the donor-like defects are removed and replaced by the positively charged compensating acceptor-like defects. This resulted in a 1.2 eV shift of the Al 2p core level towards lower binding energy. However, the C 1s core level did not change. Apparently the initial Al_2O_3 layers prevent the interface reactions during the oxygen plasma process. The conductivity of the diamond surface may slightly degrade due to the changes of the charge transfer state within the oxide and interface layers. The charge configuration and band alignment after additional PEALD Al_2O_3 deposition is presented in Fig. 6(iv).

V. CONCLUSION

In this research, surface conductive diamond was achieved with Al_2O_3 employed as a dielectric layer deposited by PEALD with a post-deposition hydrogen plasma treatment. The change of surface conductivity is monitored *in situ* using the C 1s core level and *ex situ* by electrical measurements. The VBO between Al_2O_3 and diamond is determined to be 2.7 eV, and the CBO is determined to be −1.5 eV. The Al_2O_3 is able to confine holes for the surface conductive diamond, enabling a diamond based FET. However, Al_2O_3 is not able to confine electrons on H-terminated diamond. The post-deposition hydrogen plasma treatment significantly affects the surface conductivity of diamond by changing the interface structure and the interface charge state. Moreover, the interface band alignment is thermally stable during an anneal at 500 °C, suggesting a charge configuration that differs from air exposed H-terminated diamond. It is proposed that a charged interface layer plays a critical role in the surface conductivity of the diamond and the band alignment of the diamond/Al_2O_3 interface.

ACKNOWLEDGMENTS

This research was supported by a grant from MIT-Lincoln Laboratories and the NSF through Grant No. DMR-1710551. We gratefully acknowledge the helpful discussions with Dr. Michael Geis, Dr. Mark Hollis, and Dr. Travis Wade of MIT-Lincoln Laboratories, and Professor Timothy Grotjohn of Michigan State University.

[1]J. Y. Tsao, S. Chowdhury, M. A. Hollis, D. Jena, N. M. Johnson, K. A. Jones, R. J. Kaplar, S. Rajan, C. G. Van de Walle, E. Bellotti, C. L. Chua, R. Collazo, M. E. Coltrin, J. A. Cooper, K. R. Evans, S. Graham, T. A. Grotjohn, E. R. Heller, M. Higashiwaki, M. S. Islam, P. W. Juodawlkis, M. A. Khan, A. D. Koehler, J. H. Leach, U. K. Mishra, R. J. Nemanich, R. C. N. Pilawa-Podgurski, J. B. Shealy, Z. Sitar, M. J. Tadjer, A. F. Witulski, M. Wraback, and J. A. Simmons, "Ultrawide-Bandgap Semiconductors: Research, Opportunities and Challenges," Adv. Electron. Mater. (in press).
[2]N. Fujimori, H. Nakahata, and T. Imai, Jpn. J. Appl. Phys., Part 1 **29**, 824 (1990).

[3]H. Sato and M. Kasu, Diamond Relat. Mater. **31**, 47 (2013).
[4]C. Pietzka, J. Scharpf, M. Fikry, D. Heinz, K. Forghani, T. Meisch, T. Diemant, R. J. Behm, J. Bernhard, J. Biskupek, U. Kaiser, F. Scholz, and E. Kohn, J. Appl. Phys. **114**, 114503 (2013).
[5]S. A. O. Russell, S. Sharabi, A. Tallaire, and D. A. J. Moran, IEEE Electron Device Lett. **33**, 1471 (2012).
[6]H. Kawarada, Jpn. J. Appl. Phys., Part 1 **51**, 090111 (2012).
[7]C. Verona, W. Ciccognani, S. Colangeli, E. Limiti, M. Marinelli, and G. Verona-Rinati, J. Appl. Phys. **120**, 025104 (2016).
[8]D. Takeuchi, M. Riedel, J. Ristein, and L. Ley, Phys. Rev. B **68**, 41304 (2003).
[9]M. T. Edmonds, C. I. Pakes, S. Mammadov, W. Zhang, A. Tadich, J. Ristein, and L. Ley, Appl. Phys. Lett. **98**, 102101 (2011).
[10]M. Riedel, J. Ristein, and L. Ley, Phys. Rev. B **69**, 125338 (2004).
[11]M. Kasu, M. Kubovic, A. Aleksov, N. Teofilov, Y. Taniyasu, R. Sauer, E. Kohn, T. Makimoto, and N. Kobayashi, Diamond Relat. Mater. **13**, 226 (2004).
[12]A. Daicho, T. Saito, S. Kurihara, A. Hiraiwa, and H. Kawarada, J. Appl. Phys. **115**, 223711 (2014).
[13]M. W. Geis, Proc. IEEE **79**, 669 (1991).
[14]K. Hirama, H. Sato, Y. Harada, H. Yamamoto, and M. Kasu, IEEE Electron Device Lett. **33**, 1111 (2012).
[15]D. Kueck, P. Leber, A. Schmidt, G. Speranza, and E. Kohn, Diamond Relat. Mater. **19**, 932 (2010).
[16]J. W. Liu, M. Y. Liao, M. Imura, H. Oosato, E. Watanabe, and Y. Koide, Appl. Phys. Lett. **102**, 112910 (2013).
[17]J. W. Liu, M. Y. Liao, M. Imura, H. Oosato, E. Watanabe, A. Tanaka, H. Iwai, and Y. Koide, J. Appl. Phys. **114**, 84108 (2013).
[18]S. A. O. Russell, L. Cao, D. Qi, A. Tallaire, K. G. Crawford, A. T. S. Wee, and D. A. J. Moran, Appl. Phys. Lett. **103**, 202112 (2013).
[19]K. G. Crawford, L. Cao, D. Qi, A. Tallaire, E. Limiti, C. Verona, A. T. S. Wee, and D. A. J. Moran, Appl. Phys. Lett. **108**, 42103 (2016).
[20]J. W. Lim and S. J. Yun, Electrochem. Solid-State Lett. **7**, 45 (2004).
[21]J. Yang, B. S. Eller, M. Kaur, and R. J. Nemanich, J. Vac. Sci. Technol. A **32**, 21514 (2014).
[22]H. Nakahata, T. Imai, and N. Fujimori, in *Proceedings of the 2nd International Symposium on Diamond Materials*, edited by A. J. Purdes, J. C. Angus, R. F. Davis, B. M. Meyerson, K. E. Spear, and M. Yoder (The Electrochemical Society, Inc., Pennington, NJ, 1991), Proceedings Vol. 91-8, p. 487.
[23]J. R. Waldrop and R. W. Grant, Appl. Phys. Lett. **68**, 2879 (1996).
[24]E. A. Kraut, R. W. Grant, J. R. Waldrop, and S. P. Kowalczyk, in *Heterojunction Band Discontinuities: Physics and Device Applications*, edited by F. Capasso and G. Margaritondo (Elsevier, New York, 1987).
[25]F. Maier, M. Riedel, B. Mantel, J. Ristein, and L. Ley, Phys. Rev. Lett. **85**, 3472 (2000).
[26]V. M. Bermudez, J. Appl. Phys. **80**, 1190 (1996).
[27]S. Tanuma, C. J. Powell, and D. R. Penn, Surf. Interface Anal. **43**, 689 (2011).
[28]J. W. Liu, M. Y. Liao, M. Imura, and Y. Koide, Appl. Phys. Lett. **101**, 252108 (2012).
[29]Y. Yang, T. Sun, J. Shammas, M. Kaur, M. Hao, and R. J. Nemanich, J. Appl. Phys. **118**, 165310 (2015).